



**HAL**  
open science

## Numerical simulation of granular platforms reinforced by geosynthetics on soft soil

Nisrine Abou Chaz, Claire Silvani, Pascal Villard, L. Briancon, Alain Nancey

► **To cite this version:**

Nisrine Abou Chaz, Claire Silvani, Pascal Villard, L. Briancon, Alain Nancey. Numerical simulation of granular platforms reinforced by geosynthetics on soft soil. 5th International Symposium on Geomechanics from Micro to Macro, Sep 2024, Grenoble, France. hal-04807313

**HAL Id: hal-04807313**

**<https://hal.science/hal-04807313v1>**

Submitted on 27 Nov 2024

**HAL** is a multi-disciplinary open access archive for the deposit and dissemination of scientific research documents, whether they are published or not. The documents may come from teaching and research institutions in France or abroad, or from public or private research centers.

L'archive ouverte pluridisciplinaire **HAL**, est destinée au dépôt et à la diffusion de documents scientifiques de niveau recherche, publiés ou non, émanant des établissements d'enseignement et de recherche français ou étrangers, des laboratoires publics ou privés.

# NUMERICAL SIMULATION OF GRANULAR PLATFORMS REINFORCED BY GEOSYNTHETICS ON SOFT SOIL

*N. Abou Chaz<sup>1,2,3</sup>, P. Villard<sup>1</sup>, C. Silvani<sup>2</sup>, L. Briancon<sup>2</sup> and A. Nancey<sup>3</sup>*

<sup>1</sup> *Univ, Grenoble Alpes, CNRS, Grenoble INP, 3SR, 38000 Grenoble, France*

<sup>2</sup> *INSA LYON, GEOMAS, 69621 Villeurbanne, France*

<sup>3</sup> *SOLMAX France, 95870 Bezons, France*

**Abstract:** A DEM-FEM coupled numerical model has been employed to analyze the behavior of a platform reinforced by geotextile (GTX) over soft soil under cyclic loading. Upon calibration, the model enabled the quantification of reinforcement mechanisms (soil confinement by GTX frictional effect and increase of loading capacity by GTX tensioned membrane effect). Initially, frictional forces dominated over the tensioned membrane effect, but as deflection accumulated with successive cycles, the latter gained prominence. Moreover, the model provided insights into the load transfer through the GTX, and its escalating involvement with each cycle.

## 1. Introduction

Poor subgrade is a widespread issue in unpaved road construction. Since the 1970s, geosynthetics (GSY) have emerged as a solution to this challenge. Depending on the type of GSY, various functions such as separation, reinforcement, and stabilization can be ensured. Reinforcement occurs when the GSY, shaped into a tensioned curve, transfers its tensile force to the anchoring point through a tensioned membrane effect. Stabilization is achieved by forming a composite material of soil and GSY, by interlocking or friction, resulting in a less deformable material than the soil alone. However, the contribution of each mechanism to structural improvement remains uncertain. Thus, the dominant mechanism is elusive, indicating the need to pursue research in this area.

To enhance comprehension of these mechanisms, a collaborative thesis project was launched and encompassed experimental and numerical investigations. The experimental phase carried out on a 1:1 scale, aimed to assess the performance of reinforcement under cyclic vertical loading [1,2] with two woven GTXs of varying tensile stiffness and two distinct base layer thicknesses (0.3 m and 0.5 m). The platform featuring a medium-thick base course (0.3 m) experienced notable settlement reduction with the incorporation of GTXs. The GTX with the highest stiffness emerged as the most effective. While the reinforced thick granular platform (0.5 m) exhibited no reduction in settlement when compared to its unreinforced counterpart. Hence, the vertical distance between the GTX and the applied loading is crucial for engaging the GTX and subjecting it to tension, thereby enabling it to fulfill its role. However, despite these results, the underlying mechanisms remained elusive. To overcome this challenge, a coupled numerical model integrating the DEM and FEM was employed and calibrated using the experimental results [1,2]. This publication provides a quantification of the relevant mechanisms, allowing the predominant mechanism to prevail.

## 2. Description of the 3D DEM-FEM coupled numerical model

The employed numerical model is a coupled system comprising discrete element methods (DEM) and finite element methods (FEM) and implemented through the Spherical Discrete Elements Code [3]. The DEM component accounts for the discrete nature of aggregate, while the FEM component

addresses the fibrous and continuous characteristics of the GTX, with coupling between DEM and FEM addressing frictional interactions at the soil-GTX interface. The model (Figure 1), comprises:

1. an arrangement of clusters representing granular behavior, interacting via contact points.
2. thin, finite triangular elements describing GTX membrane behavior and tension.
3. a layer of spheres associated with springs representing supporting soil, moving only vertically.

Horizontal and vertical frictionless walls delineate boundary conditions, while a circular rigid plate (Diameter=0.3 m) applies vertical load at the center of the model.

The granular platform features various intergranular parameters [angularity ( $Ang$ ), porosity ( $n$ ), intergranular friction angle ( $\phi_{int}$ ), and adhesion ( $a$ )]. Clusters interact via contact points based on the molecular dynamic method. Furthermore, each triangular element modeling the GTX consists of fibers with varying orientations. The behavior of the fiber network is obtained through superimposing behaviors of each fiber direction. Furthermore, fibers sharing the same direction adhere to specific behavior laws, with fiber stiffness ( $J$ ) correlating tensile force ( $T$ ) to deformation ( $\epsilon$ ). A contact law akin to DEM between grains describes the interaction between clusters and triangular finite elements. Interaction contact forces are determined based on updated overlaps at each  $\Delta t$ .

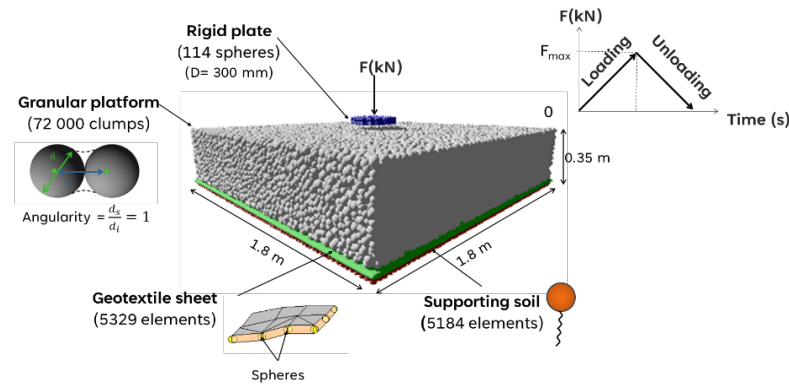


Figure 1. Geometry of the numerical model

### 3. Confrontation between the numerical model and the experimental setup

Ensuring alignment between the numerical model and experimental tests involves harmonizing the macroscopic characteristics of the cluster assembly of the numerical model with those of the gravel utilized in the experiments. Micro-mechanical parameters of the cluster assembly ( $n$ ,  $Ang$ ,  $\phi_{int}$ ,  $a$ ) were adjusted to align both the macroscopic friction angle ( $\phi_{peak}$ ) and cohesion ( $c$ ) shear tests conducted on the gravel used in the experiment. Numerical triaxial tests on the cluster assembly have been carried out to reproduce the micromechanical parameters obtained experimentally (Table 1). Furthermore, friction parameters at the interface between GTX and the lower subgrade or upper granular platform (Table 1) were determined by direct shear tests using a  $0.2 \times 0.2 \times 0.2 \text{ m}^3$  test box. Moreover, tensile tests on the GTX revealed a linear behavior law governing tensile force ( $T$ ) and deformation ( $\epsilon$ ), with one slope ( $J$ ) representing the stiffness for both the x and y directions (Table 1). An experimental cyclic plate load test was conducted to obtain the modulus evolution of the subgrade soil with cycles. During loading cycles, the soil modulus increased, while it remained approximately constant during unloading. After a certain number of cycles, the soil transitioned from plastic to elastic behavior, as indicated by an equilibrium between loading and unloading moduli. These observations informed the development of a simplified behavioral law (1):

$$k_N = \begin{cases} k_1 + \frac{N-1}{N_0}(k_u - k_1) \\ k_u \end{cases} \quad (1)$$

where  $k_N$  represents the rigidity of the  $N^{\text{th}}$  loading cycle,  $k_1$  is the rigidity of the 1<sup>st</sup> loading cycle,  $k_u$  is the rigidity of all unloading cycles,  $N$  denotes the cycle number applied, and  $N_0$  is the threshold cycle number at which the subgrade soil became elastic. The soil parameters were calibrated to match subgrade soil settlement in the experimentation after 1000 cycles to settlement in the numerical model after a reduced number of cycles (30 cycles), thus optimizing computational efficiency (Table 1).

Following the application of 30 loading cycles on the circular plate with a maximum applied load of 40 kN (560 kPa), the calibrated model exhibits a notable convergence with experimental data, as outlined [1,2]. Specifically, the calibrated model accurately replicates the range of displacement and stress observed in one of the experimental tests after both the 1<sup>st</sup> and the last cycles. The next section will delve into the relevant mechanisms and the role of the GTX in loading transfer.

Table 1 . Numerical parameters describing the different components of the model

Angularity	$Ang$	1
Porosity	$n$	0.38
Intergranular friction angle (°)	$\phi_{int}$	20
Adhesion (kPa)	$a$	25
Peak friction macroscopic angle (°)	$\phi_{peak}$	39
Cohesion (kPa)	$c$	13.5
<b>GTX</b> tensile stiffness in the x and y directions (kN/m) [ 0 - 5% strain]	$J_x \& J_y$	1200
Angle between the clumps and the upper <b>interface</b> of the GTX (°)	$\Phi_{clumps-GTX}$	38
Angle between the supporting and the lower <b>interface</b> of the GTX (°)	$\Phi_{sphere-GTX}$	32
<b>Subgrade</b> reaction modulus during the 1 <sup>st</sup> loading (MPa/m)	$k_1$	2
<b>Subgrade</b> reaction modulus during the unloading (MPa/m)	$k_u$	100
Threshold cycle number	$N_0$	30

#### 4. Relevant mechanisms and load transfer through the tensioned membrane effect

In the numerical model, access to the forces corresponding to the relevant mechanisms is provided. The studied segment of the GTX lies in the middle of the model, aligned with the y-direction, and extends over a width of 0.1 m along the x-direction (Figure 2). In the y-direction, the tangential forces exerted by the clusters on the GTX finite elements are denoted by  $ft_2$ , while the tensile forces within the GTX itself are represented by  $T_2$ .  $ft_2$  characterizes the friction mechanism, while the resulting between  $ft_2$  and  $T_2$  within the GTX quantifies the effects attributed to the tensioned membrane effect. During the 1<sup>st</sup> loading cycle, the taut membrane effect takes precedence under the plate, while friction dominates around the plate projection. During subsequent cycles, the friction force profiles show relative constancy, particularly from the 1<sup>st</sup> cycle to the 30<sup>th</sup> cycle, while the force associated with the tensioned membrane increases, with significant growth from the 1<sup>st</sup> cycle to the 30<sup>th</sup> cycle. Consequently, the 1<sup>st</sup> cycle highlights the importance of the friction effect. However, as the cycles progress and the deformation and deflection of the GTX intensify, the effect of the tensioned membrane overcomes the effect of friction, eventually dominating it in subsequent cycles.

Furthermore, Figure 3 shows the difference in vertical stress ( $\Delta\sigma$ ) on the upper face of the GTX from the lower face after the 1<sup>st</sup> and 30<sup>th</sup> loading cycles. A negative value  $\Delta\sigma$  is showed in a circular area centered on the center point of the loading plate, with a diameter  $D_1 = 2D$  ( $D = 0.3$  m). Conversely, it shows a positive value in the region between circles of diameter  $D_1 = 2D$  and  $D_2 = 4D$ . This indicates that part of the stress on the upper face of the GTX is directly transferred to the subgrade, while another part is transmitted by the GTX itself to the surrounding area through the

tensioned membrane effect. Furthermore, the  $\Delta\sigma$  amplitudes between the 1<sup>st</sup> and 30<sup>th</sup> loading cycles becomes increasingly pronounced indicating that the GTX contributes progressively more to load distribution through membrane effects with the accumulation of deflection and strain within the GTX.

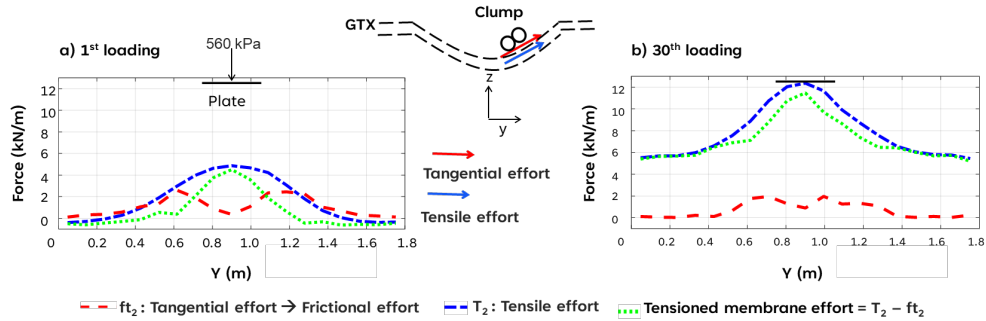


Figure 2. The relevant mechanisms after the: a) 1<sup>st</sup> & b) 30<sup>th</sup> loading

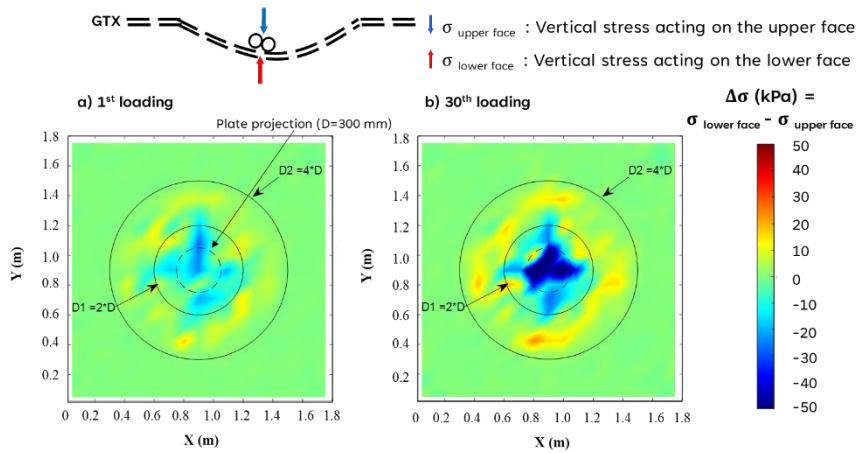


Figure 3. The resultant of vertical stress acting on the GTX after a) the 1<sup>st</sup> & b) the 30<sup>th</sup> loading

## 5. Conclusions

Following calibration of the FEM-DEM 3D model to match the range of experimental settlements, it showed accurate in reproducing the range of stresses observed [1,2]. During the 1<sup>st</sup> cycle, the friction mechanism outweighs the tensioned membrane effect, but as deflection increases with cycles, the tensioned membrane takes on greater prominence. These dynamics revealed an increasing dominance of the reinforcement role over the stabilization role by confinement. Moreover, the model revealed valuable insights into load transfer by the GTX, highlighting its increasing engagement with cycles.

## References

- [1] Abou Chaz N., Briançon L., Villard P., Silvani C., Nancey A., Abdelouhab A. (2023). *Experimental and numerical studies of the geosynthetics reinforced platforms laid over soft subgrade soil*. 3S Web of Conferences 368, 7p.
- [2] Abou Chaz N. (2024). *Experimental and Numerical studies of granular platforms reinforced by geosynthetics laid over soft subgrade soil*. PhD thesis, Grenoble Alpes university, 205 p.
- [3] Villard P., Chevalier B., Le Hello B. & Combe G. (2009). *Coupling between finite and discrete element methods for the modelling of earth structures reinforced by geosynthetics*. Computers and Geotechnics, 36, pp. 709-717.